INL/CON-22-67800-Revision-0

ANS Winter 2022: ATF-2C Physics Safety and Scoping Analysis

November 2022

Changing the World's Energy Future

Travis J Labossiere-Hickman, Andrew John Bascom, Brian P Durtschi, David W Kamerman

Idaho National Laboratory

INL/CON-22-67800-Revision-0

ANS Winter 2022: ATF-2C Physics Safety and Scoping Analysis

Travis J Labossiere-Hickman, Andrew John Bascom, Brian P Durtschi, David W Kamerman

November 2022

Idaho National Laboratory
Idaho Falls, Idaho 83415

http://www.inl.gov

Prepared for the
U.S. Department of Energy
Under DOE Idaho Operations Office
Contract DE-AC07-05ID14517

ATF-2C Physics Safety and Scoping Analysis

Travis Labossiere-Hickman, Andrew Bascom, Brian Durtschi, David Kamerman

Idaho National Laboratory, 2525 North Fremont Avenue, Idaho Falls, ID, United States
Travis.LabossiereHickman@INL.gov, Andrew.Bascom@INL.gov, Brian.Durtschi@INL.gov, David.Kamerman@INL.gov

INTRODUCTION

Background

Following the accident at the Fukushima Daiichi nuclear power plant in 2011, the accident tolerant fuels (ATF) program was created to research and develop safer light-water reactor (LWR) fuels [1] with a particular emphasis on cladding. Prerequisite for the wide-scale deployment of ATF in commercial reactors is irradiation testing of the fuel designs. ATF-2C is the latest in the series of of ATF experiments irradiated in the Advanced Test Reactor (ATR) at Idaho National Laboratory (INL). Prior to insertion, extensive physics safety analysis must show compliance with the safety analysis report (SAR) [2] and customer requirements under a series of bounding assumptions.

About the Experiment

ATF-2C comprises four tiers with six rodlets each. The experiment test train (TT) is situated in Loop 2A in the center flux trap (CFT) of the ATR, in which typical pressurized water reactor (PWR) conditions shall be approximated. Tier 1 (bottom) of the TT tests Framatome silicon carbide (SiC) cladding, containing molybdenum heater rods. Low-enriched uranium (LEU) Framatome rodlets with chrome-coated M5 cladding have been modeled in their place for the physics safety analysis to allow the substitution of this tier with fuel if needed. Tier 2 tests LEU Framatome rodlets with M5 cladding, which had irradiated in ATR in prior ATF experiments. Tier 3 tests General Atomics SiC composite cladding, also containing molybdenum heater rods. Tier 4/5/6 (top) tests the Japan Atomic Energy Agency (JAEA)/Mitsubishi Heavy Industries (MHI) fueled rodlets. This upper tier tests LEU rodlets with chrome-coated MDA cladding—several with temperature or pressure instrumentation. To flatten the axial power profile, lower portion of Tier 4/5/6 is surrounded by a hafnium (Hf) shroud, and the bottom two UO_2 pellets are of natural enrichment. The ATF-2C TT is to be irradiated in the CFT of ATR (Fig. 1) for three or four 60-day cycles.

CODES AND METHODS

Modeling Assumptions

To allow for customer flexibility, operational flexibility, and last-minute changes, bounding assumptions are applied to the experiment configuration. For example, Tier 1, and Tier 2, and the Tier 4/5/6 natural-uranium pellets are modeled as fresh LEU. This permits the substitution of these rodlets and pellets within the envelope of the safety calculations.

The UO_2 pellet stacks are modeled as continuous cylinders with no dishes or chamfers, which conservatively overestimates fuel volume. Loop 2A moderator is modeled without boron, whereas the actual loop chemistry typically contains $\approx$ 1000 ppmb. The H-positions immediately outside the CFT (Fig. 2) are modeled containing high specific activity (HSA) cobalt, which is less absorptive than other likely isotope production targets.

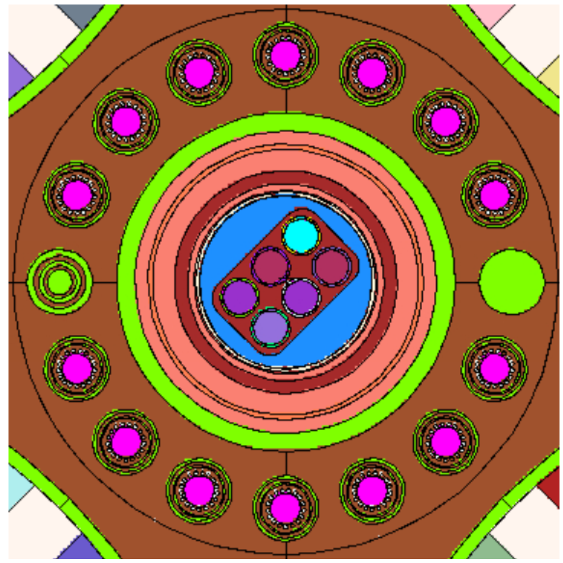

Fig. 1. ATF-2C in the CFT.

ATR irradiation experiment analyses are generally modeled as fixed-source problems using a characteristic fission source in the reactor driver fuel [3]. Lobes operate in the vicinity of 20 MW during normal operation. For a bounding safety case, a representative early-cycle lobe power split is chosen with the center lobe increased to 25 MW. This bounds all conceivable steady-state operational conditions. An additional 2σ lobe power uncertainty of 8.5% [4] and fabrication uncertainty of 5% are applied on top of the safety-basis heating rates. Combining these by summing the variances [5] leads to a 2σ uncertainty of 9.86%.

Codes

Neutron transport and reaction rate calculations were performed using MCNP6.2 [6]. Depletion calculations for material damage projections were performed using ORIGEN2.2 [7]. Calculations were performed at the INL High Performance Computing Center.

Normalization Method

To convert per-source-particle tally results to absolute neutron fluxes and reaction rates, it is necessary to normalize to the average neutrons per fission ν, average energy per fission

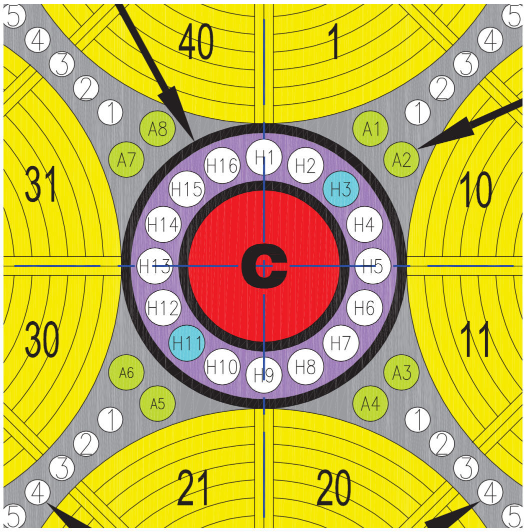

Fig. 2. Schematic of the ATR CFT, H-positions, and adjacent driver fuel elements.

ε, and core power observed by the lobe (i.e., lobe-adjusted total core power [LATCP]). The five lobes of the ATR—northwest, northeast, center, southwest, and southeast—are largely but not entirely independent of one another. The LATCP itself serves to normalize the reaction rates in a given lobe given the overall lobe power distribution. See Eq. 1 for the LATCP calculation given planned power Q_L, tally result $(f7:n)_L$, and tally mass m_L:

$$LATCP(L) = \frac{Q_L}{(f7:n)_L \times m_L} \sum_{i=1}^{5} (f7:n)_i m_i \tag{1}$$

Flux Calculations

Neutron flux calculations were performed using $f4$ tallies as shown in Eq. 2.

$$\phi = \frac{\nu}{\varepsilon}(LATCP)(f4:n) \tag{2}$$

For thermal fission in ^{235}U, ν/ε is conservatively assumed to be 0.01215 fission neutrons per MeV [3].

In this document, we shall bin energy groups as follows: 0 eV < thermal ≤ 0.625 eV < epithermal ≤ 1 MeV < fast.

Heating Rate Calculations

Heating rates calculations are similar to fluxes, but they are performed using $f7$ tallies (MeV/g) multiplied by masses (Eq. 3):

$$Q = \frac{\nu}{\varepsilon}(LATCP)(f7:n) \times m \tag{3}$$

Material Damage Calculations

A multiplier may be applied to an $f4$ tally to obtain a reaction rate. For a given material, we may apply the NJOY total damage-energy cross-section [8] (reaction 444). The rate of displacements per atom (DPA) may be calculated from the damage-energy tally using the Norgett-Robinson-Torrens model [9]. This gives us Eq. 4, where η is the displacement efficiency (≈ 80%), E_d is the average displacement threshold energy, and $\sigma_{d,x}(E)\phi_x(E,t)$ is the damage-energy reaction rate:

$$\frac{\partial D_x}{\partial t} = \frac{\eta}{2E_d} \int_0^\infty \sigma_{d,x}(E)\phi_x(E,t)dE \tag{4}$$

E_d is material-dependent and not well characterized. For zirconium, a value of 40 ± 8 eV is recommended by Konobeyev et al. [10]; the mean value shall be used as a proxy for the MDA zirconium alloy. The DPA rate may then be calculated according to Eq. 5:

$$\frac{\partial}{\partial t}DPA = \frac{\nu}{\varepsilon}(LATCP)\frac{\eta}{2E_d}(f4:n,444) \tag{5}$$

RESULTS

Base Case with Shroud

The total fission power of ATF-2C shall not exceed 200 kW, as per the SAR [2]. Given the conservative approximations described previously and the safety-case lobe power split, we find that the shrouded ATF-2C design is well within the safety limits. See Table II.

TABLE I. ATF-2C Fission Power with Shroud

Tier	Nominal Power (kW)	Safety-Case Power (kW)	Safety-Case $+2\sigma$ (kW)
4/5/6	81.57	94.40	103.7
2	25.08	29.03	31.89
1	20.87	24.15	26.53
Total	127.51	147.58	162.13

The impact of the Tier 4/5/6 Hf shroud can be clearly seen in the lower 24 cm of the average linear heat generation rate (LHGR) and flux plots, shown in Figs. 3 and 4, respectively. The thermal flux is more important for power and burnup, whereas the fast flux > 1 MeV mainly drives material damage.

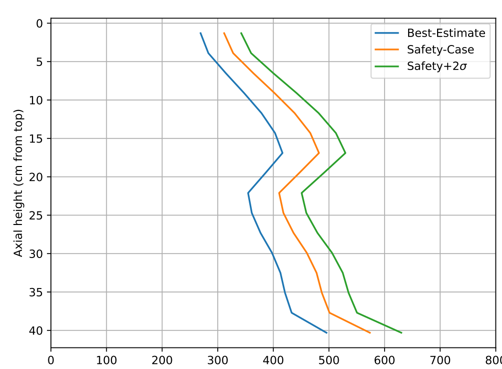

Fig. 3. Tier 4/5/6 LHGRs with Hf shroud.

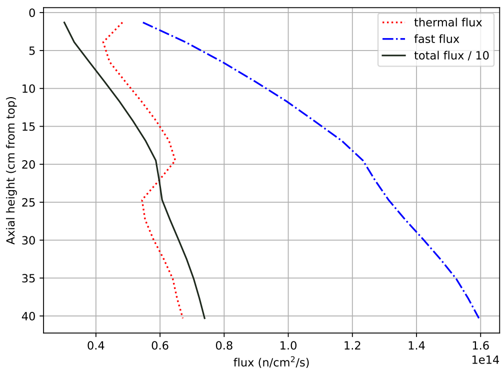

Fig. 4. Tier 4/5/6 nominal cladding flux with shroud. Total flux has been scaled to 10% for visibility.

The material damage accumulation was projected for three full-power 60-day cycles of ATR operation. By the end of the third cycle of irradiation, the cladding sample is expected to peak at ≈ 3–4 DPA (Fig. 5).

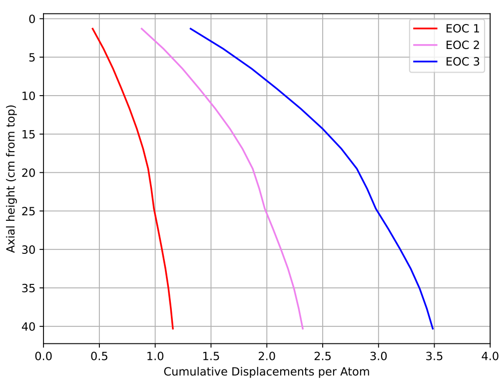

Fig. 5. Tier 4/5/6 end of cycle (EOC) projected DPA.

Case without Shroud

Due to supply chain concerns, it was necessary to evaluate a scenario in which the custom-manufactured Hf shroud could not be delivered. As the shroud reduces power in the experiment, such a situation is not bounded by the base safety analysis. The two natural-enrichment pellets at the bottom of Tier 4/5/6 were reintroduced into the model, and three alternatives were examined: (1) Hf pellets in place of UO_2 in the two center rodlets; (2) Nitronic-60 shroud; and (3) no shroud or Hf.

Note the effect of the natural-enrichment pellets at the bottom of Figs. 6 and 7.

TABLE II. ATF-2C Total Fission Powers without Hf Shroud

Case	Nominal Power (kW)	Safety-Case Power (kW)	Safety-Case $+2\sigma$ (kW)
Hf pellets	102.02	118.08	129.73
Nitronic-60	145.67	168.60	185.23
No shroud/Hf	148.58	171.97	188.93

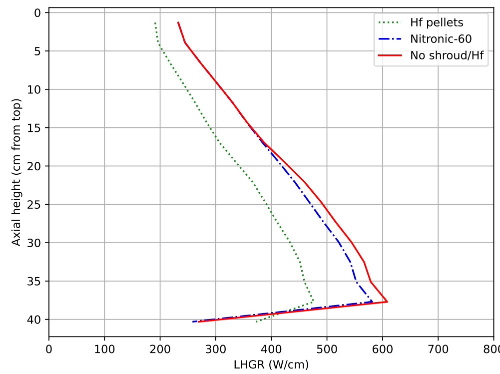

Fig. 6. Tier 4/5/6 nominal LHGRs without Hf shroud.

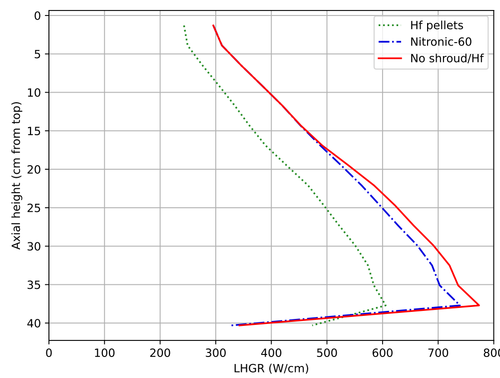

Fig. 7. Tier 4/5/6 safety-case $+2\sigma$ without Hf shroud.

The Hf pellet option, while not as effective as the original design, is the most effective of the three alternatives. Unfortunately, it sacrifices two fueled rodlets. The second option, replacing the lower shroud with one made of Nitronic-60, has a small but non-negligible advantage. It reduces the peak LHGR by around 5% from the design with no shroud or Hf. Nevertheless, even that most limiting case remains inside the 200 kW safety limit.

CONCLUSIONS

ATF-2C is safe for insertion under the most limiting conditions. The lower Hf shroud should be used if possible. Several alternatives are available if it is not, with a substitute Nitronic shroud having the fewest downsides.

The greatest source of numeric uncertainty is the measured ATR lobe power. A 2σ uncertainty of 8.5% limits the acceptable design space. Work is ongoing at INL to better quantify this lobe power uncertainty [11].

Bounding safety calculations allow this analysis to bound a variety of experiments. The calculations described in this paper bound the later cycles of irradiation, alternate ATF-2C configurations, and a number of future ATF experiments. Future work for ATF-2D and onward shall examine a new safety model with a fueled Tier 3.

The final takeaway from the ATF-2C physics safety and scoping analysis is that the greatest source of uncertainty is not necessarily numeric. The potential unavailability of a key component required additional safety analysis outside the original envelope. In these uncertain times, planning for supply chain shortcomings in nuclear safety calculations may need to become standard practice.

ACKNOWLEDGMENTS

This work was supported through the U.S. Department of Energy Advanced Fuels Campaign under DOE Idaho Operations Office Contract DE-AC07-05ID14517. Accordingly, the U.S. Government retains and the publisher, by accepting the article for publication, acknowledges that the U.S. Government retains a nonexclusive, paid-up, irrevocable, world-wide license to publish or reproduce the published form of this manuscript, or allow others to do so, for U.S. Government purposes.

This research made use of the resources of the High Performance Computing Center at Idaho National Laboratory, which is supported by the Office of Nuclear Energy of the U.S. Department of Energy and the Nuclear Science User Facilities under Contract No. DE-AC07-05ID14517.

REFERENCES

1. J. CARMACK, F. GOLDNER, S. M. BRAGG-SITTON, and L. L. SNEAD, "Overview of the US DOE accident tolerant fuel development program," Tech. rep., Idaho National Laboratory, Idaho Falls, ID (United States) (2013).
2. SAR-153, "Chapter 10 – Experiments and Irradiation Facilities – Upgraded Final Safety Analysis Report for the Advanced Test Reactor," Revision 31," Tech. Rep. SAR-153, Idaho National Laboratory (2021).
3. GDE-594, "Experiment Design and Analysis Guide: Neutronics Physics," Tech. Rep. GDE-594, Idaho National Laboratory (2017).
4. GDE-588, "Thermal-Hydraulic Analysis Team (THAT) Guidebook," Tech. Rep. GDE-588, Idaho National Laboratory (2020).
5. G. F. KNOLL, *Radiation Detection and Measurement*, John Wiley & Sons, Inc., 3rd ed. (2000).
6. C. J. WERNER ET AL., "MCNP6.2 Release Notes," Tech. Rep. LA-UR-18-20808, Los Alamos National Laboratory (2018).
7. S. LUDWIG and A. CROFF, "Revision to ORIGEN2– version 2.2," *Transmittal memo of*, **300**, *0371*, 17 (2002).
8. R. MACFARLANE, D. W. MUIR, R. M. BOICOURT, A. C. KAHLER, III, and J. L. CONLIN, "The NJOY Nuclear Data Processing System, Version 2016," .
9. M. NORGETT, M. ROBINSON, and I. TORRENS, "A proposed method of calculating displacement dose rates," *Nuclear Engineering and Design*, **33**, *1*, 50–54 (1975).
10. A. KONOBEYEV, U. FISCHER, Y. KOROVIN, and S. SIMAKOV, "Evaluation of effective threshold displacement energies and other data required for the calculation of advanced atomic displacement cross-sections," *Nuclear Energy and Technology*, **3**, *3*, 169–175 (2017).
11. N. H. MANWARING, "Power Uncertainty for Advanced Test Reactor Experiment Analyses," Tech. Rep. ECAR-4760, Idaho National Laboratory (2020).